Electronic Supplementary Information

Thermodynamic Properties and Molecular Dynamics of $[Li^+@C_{60}](PF_6^-)$
Associated with Structural Phase Transitions

Hal Suzuki,[1] Misaki Ishida,[2,3] Chiko Otani,[2,3] Kazuhiko Kawachi,[4] Yasuhiko Kasama,[4] Eunsang Kwon,[5] Yuji Miyazaki,[6] Motohiro Nakano[6]

1. Department of Chemistry, Kindai University, 3-4-1 Kowakae, Higashiosaka, Osaka 577-8502, Japan
2. Department of Physics, Graduate School of Science, Tohoku University, 6-3 Aramaki-Aoba, Sendai, Miyagi 980-8578, Japan
3. Terahertz Sensing and Imaging Research Team, RIKEN Center for Advanced Photonics, RIKEN, 519-1399 Aramaki-Aoba, Sendai, Miyagi 980-0845, Japan
4. Idea International Co. Ltd., Sendai, Miyagi 980-8579, Japan
5. Research and Analytical Center for Giant Molecules, Graduate School of Science, Tohoku University, Sendai, Miyagi 980-8578, Japan
6. Research Center for Thermal and Entropic Science, Graduate School of Science, Osaka University, Toyonaka, Osaka 560-0043, Japan

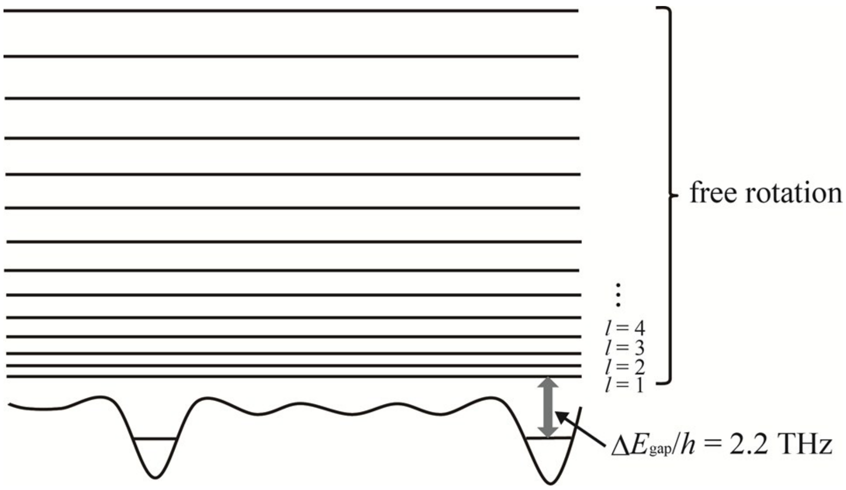

Fig. S1 A simple energy scheme with respect to the Li^+ rotational states for $[Li^+@C_{60}](PF_6^-)$ proposed in the previous work. [1] Two localized ground levels lie beneath free rotation levels.

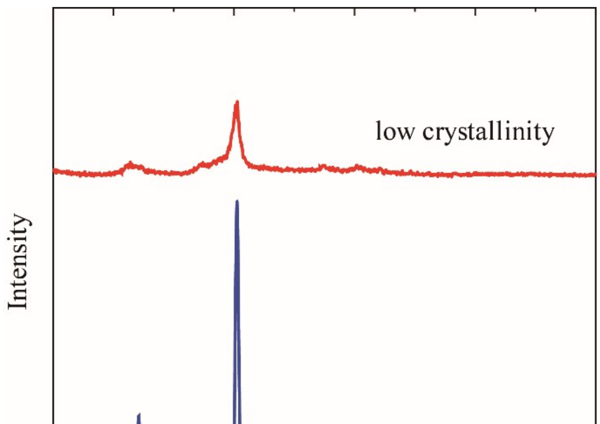

Fig. S2 Powder XRD pattern of $[Li^+@C_{60}](PF_6^-)$ crystals. The sample measured in this study (high crystallinity) shows sharp Bragg peaks (blue), while that with low crystallinity shows diffused peaks (red).

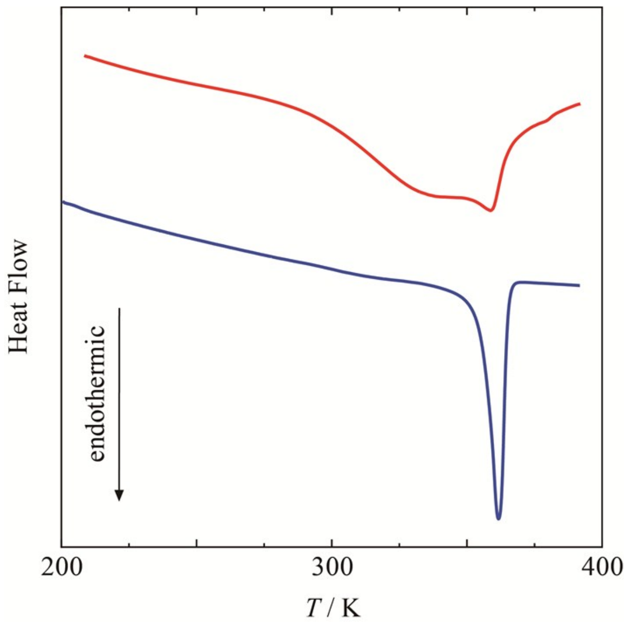

Fig. S3 DSC curves of $[Li^{+}@C_{60}](PF_6^{-})$ crystals between 200 and 400 K (heating measurements). The sample measured in this study (high crystallinity) shows a sharp transition peak at 360 K (blue), while the sample with low crystallinity shows broad peaks (red). The measurements were conducted by using X-DSC7000 (SII) with scanning rate of $dTdt^{-1} = 10$ K min^{-1}.

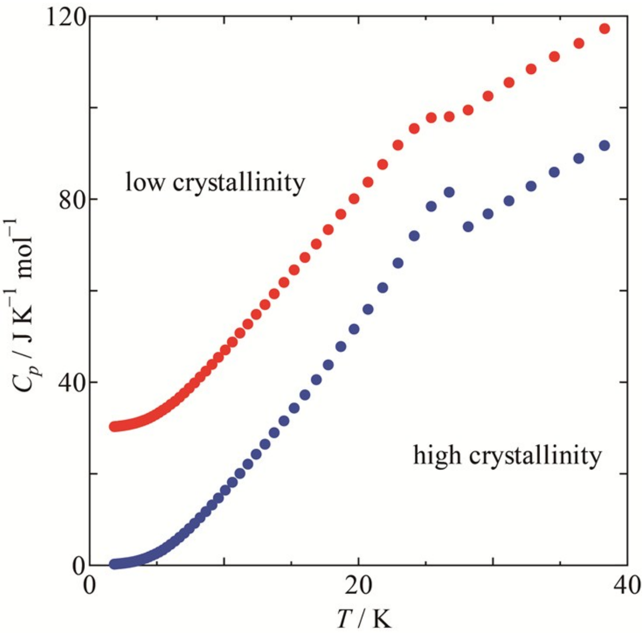

Fig. S4 C_p of $[Li^{+}@C_{60}](PF_6^{-})$ between 1.8 and 40 K obtained by relaxation calorimetry. The sample measured in this study (high crystallinity) shows a clear transition peak at 24 K (blue), while the sample with low crystallinity shows broad peak (red). The data for the sample with lower crystallinity are shifted upward by 30 J K^{-1} mol^{-1}.

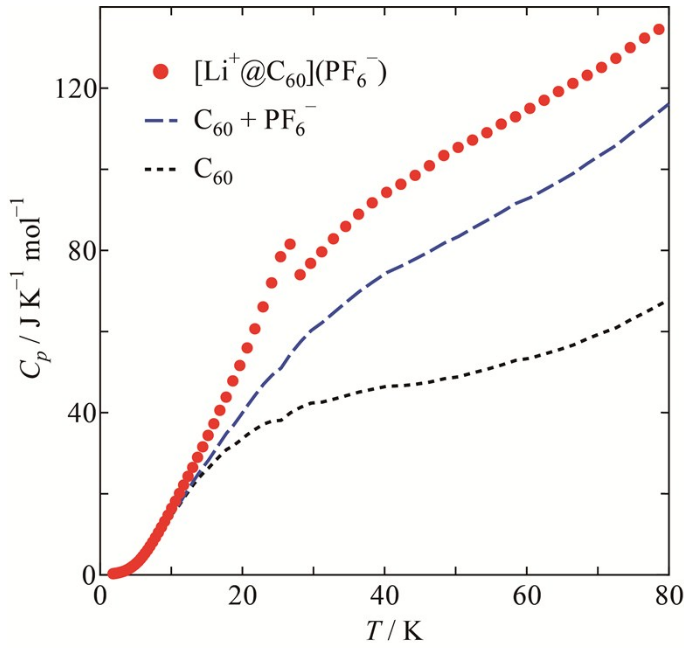

Fig. S5 C_p of $[Li^+@C_{60}](PF_6^-)$, pristine C_{60} and $C_{60}+PF_6^-$ between 1.8 and 80 K (red marks). The data of pristine C_{60} is the experimental data reported past.[2] The C_p of PF_6^- is calculated by using Einstein model.

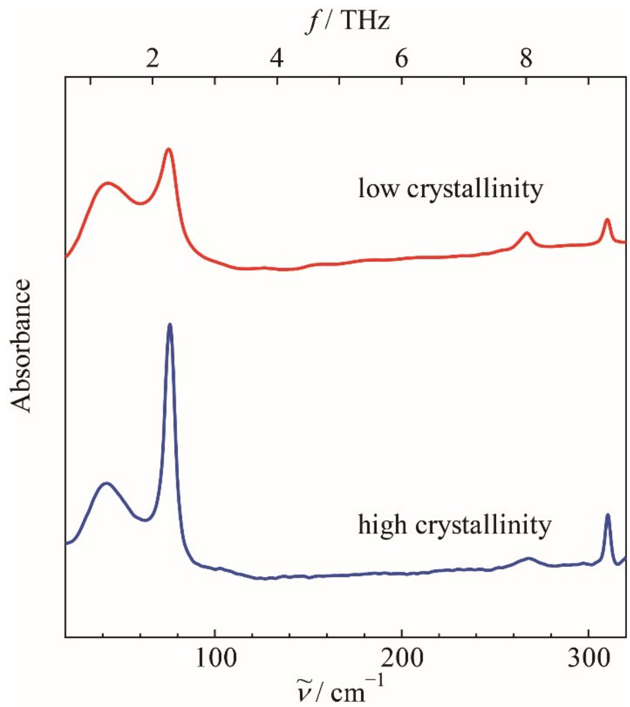

Fig. S6 THz-FIR spectra of $[Li^+@C_{60}](PF_6^-)$ crystals at 300 K. The sample measured in this study (high crystallinity) shows a sharp peak at 76 and 310 cm^{-1}, while the sample with low crystallinity shows broad peaks.

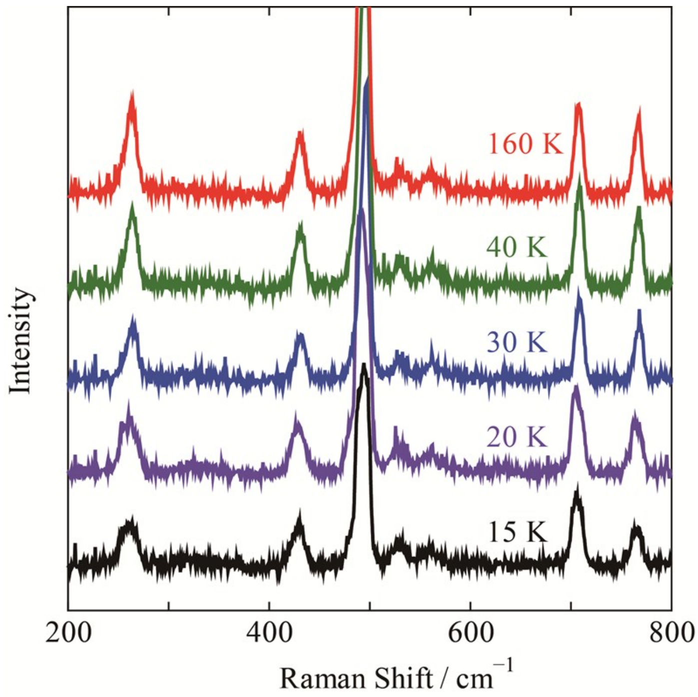

Fig. S7 Raman spectra of $[Li^+@C_{60}](PF_6^-)$ obtained at 15 – 160 K in the wavenumber range from 200 to 800 cm^{-1}. The peak intensities at 260 and 760 cm^{-1} decrease with decreasing temperature. The measurements were conducted by using NR-100 spectrometer (JASCO) equipped with Ar laser and CCD detector.

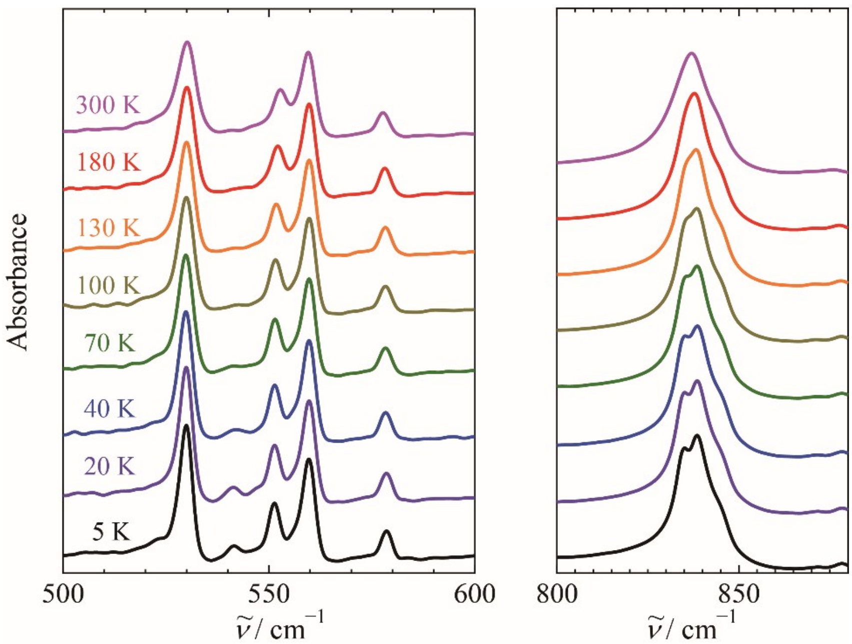

Fig. S8 IR spectra of $[Li^+@C_{60}](PF_6^-)$ at 5 – 300 K in the wavenumber range (a) from 500 to 600 cm^{-1}, and (b) from 800 to 880 cm^{-1}.

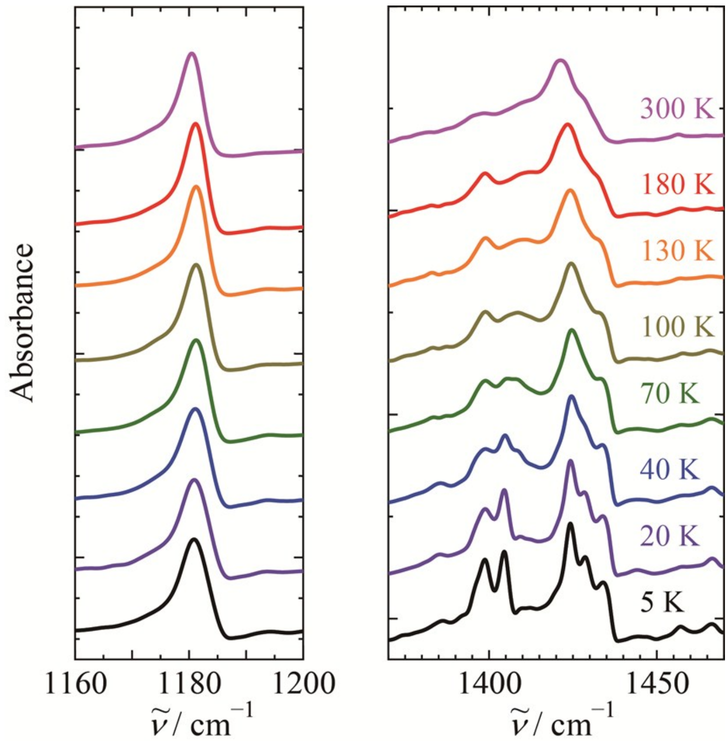

Fig. S9 IR spectra of $[Li^{+}@C_{60}](PF_6^{-})$ at 5 – 300 K in the wavenumber range (a) from 1160 to 1200 cm^{-1}, and (b) from 1370 to 1470 cm^{-1}.

Table S1 Experimental molar heat capacities of $[Li^+@C_{60}](PF_6^-)$ obtained by relaxation calorimetry.

T / K	C_p / J K^{-1} mol^{-1}	T / K	C_p / J K^{-1} mol^{-1}	T / K	C_p / J K^{-1} mol^{-1}
1.87	0.17	9.14	13.10	42.36	96.20
1.97	0.20	9.62	14.61	44.37	98.39
2.07	0.22	10.12	16.32	46.39	100.77
2.18	0.25	10.65	18.06	48.40	103.30
2.29	0.28	11.21	19.98	50.42	105.28
2.41	0.32	11.80	22.02	52.44	107.10
2.54	0.37	12.42	24.18	54.46	108.92
2.67	0.41	13.08	26.38	56.47	111.04
2.82	0.48	13.76	28.88	58.49	112.83
2.96	0.54	14.49	31.46	60.50	114.92
3.12	0.62	15.25	34.27	62.52	116.90
3.28	0.71	16.05	37.14	64.53	119.07
3.45	0.82	16.89	40.46	66.55	121.06
3.63	0.95	17.78	43.71	68.57	123.07
3.82	1.11	18.72	47.71	70.59	125.01
4.02	1.30	19.70	51.51	72.60	127.25
4.24	1.51	20.74	55.85	74.62	129.89
4.46	1.78	21.83	60.56	76.64	132.25
4.70	2.09	22.97	65.96	78.65	134.40
4.95	2.42	24.18	71.89	80.67	136.83
5.20	2.83	25.44	78.33	82.69	139.77
5.48	3.27	26.78	81.43	84.71	142.08
5.76	3.85	28.19	73.89	86.72	144.55
6.06	4.49	29.67	76.70	88.74	147.27
6.38	5.21	31.23	79.54	90.76	150.20
6.72	6.04	32.87	82.75	92.78	153.39
7.07	6.94	34.59	85.80	94.79	156.97
7.45	7.96	36.41	88.81	96.81	160.56
7.84	9.10	38.32	91.62	98.82	163.94
8.25	10.33	40.34	93.49	100.84	166.62
8.68	11.65	40.35	94.20		

Table S2 Experimental molar heat capacities of $[Li^+@C_{60}](PF_6^-)$ obtained by adiabatic calorimetry.

T / K	C_p / J K^{-1} mol^{-1}	T / K	C_p / J K^{-1} mol^{-1}	T / K	C_p / J K^{-1} mol^{-1}
Series 1		361.66	1083.8	235.47	524.3
248.42	560.2	363.69	947.1	240.44	533.0
252.40	567.2	365.73	856.7	245.41	556.0
257.37	578.6	367.79	860.5	250.38	562.6
262.34	597.3	369.85	863.2	255.35	575.2
267.30	609.7	372.37	871.3	260.31	589.2
272.26	622.5	375.34	877.4	265.28	606.2
277.23	636.2	378.30	886.4	270.24	623.7
282.19	651.7	381.26	891.4	275.21	629.9
287.15	672.4	384.22	897.9	280.17	645.9
292.11	693.1	387.18	906.3	285.13	665.7
297.07	700.1	390.13	912.7	290.09	686.1
302.03	717.2	Series 2		295.05	697.8
306.98	736.4	141.28	261.3	300.01	710.9
311.93	754.6	146.20	270.0	304.96	727.6
316.88	777.1	151.14	282.3	309.92	749.1
321.83	800.9	156.08	300.7	314.88	765.6
326.78	834.8	161.03	316.4	319.83	793.8
331.72	878.4	165.98	328.4	324.78	821.7
336.66	924.6	170.93	344.8	329.73	864.7
340.12	958.7	175.89	358.7	334.67	906.0
342.09	980.8	180.84	376.1	339.62	961.4
344.06	1002.2	185.81	379.9	344.56	1023.6
346.03	1050.5	190.77	401.5	349.49	1223.5
348.01	1116.0	200.71	430.2	354.33	1819.4
349.98	1237.4	205.68	444.7	359.27	1319.4
351.93	1454.6	210.64	454.7	364.35	912.0
353.86	1736.1	215.61	462.1	369.36	859.4
355.77	1993.6	220.58	477.7	374.31	874.4
357.69	1675.4	225.54	493.6	379.24	888.0
359.65	1187.6	230.51	504.1	384.17	896.7

Table S2 (Continued)

T / K	C_p / J K^{-1} mol^{-1}	T / K	C_p / J K^{-1} mol^{-1}	T / K	C_p / J K^{-1} mol^{-1}
389.10	911.4	360.77	1104.8	330.21	861.1
Series 3		362.79	1002.7	335.16	905.9
251.50	565.5	364.82	858.6	338.61	945.3
256.47	573.5	366.88	858.1	340.57	962.8
261.44	592.5	368.94	859.4	342.53	987.5
266.40	604.7	371.00	871.2	344.49	1014.4
271.37	621.2	373.51	874.1	346.46	1050.4
276.33	637.5	376.47	877.0	348.43	1129.5
281.30	647.2	379.43	888.1	350.39	1257.4
286.26	665.0	382.39	896.3	352.33	1467.8
291.22	686.8	385.35	900.4	354.25	1805.9
296.19	697.8	388.30	910.8	356.15	2022.7
301.14	717.1	391.25	914.8	358.06	1525.3
306.10	732.5	394.20	924.0	360.04	1154.3
311.06	751.2	Series 4		362.04	1045.6
316.02	771.4	251.69	561.8	364.07	906.7
320.97	799.7	255.89	570.2	366.11	861.3
325.92	827.3	260.85	588.4	368.17	860.8
330.86	875.1	265.81	603.2	370.22	867.5
335.81	911.5	270.77	619.2	372.73	874.8
339.26	941.2	275.73	633.2	375.70	881.3
341.23	973.4	280.69	645.5	378.66	887.3
343.20	992.4	285.65	665.1	381.62	891.5
345.17	1034.4	290.61	682.5	384.57	897.0
347.14	1071.1	295.56	695.4	387.53	908.3
349.12	1155.1	300.52	711.9	390.49	909.2
351.08	1301.8	305.47	728.6	Series 5	
353.02	1580.4	310.42	748.0	251.91	562.2
354.94	1891.6	315.37	771.2	256.88	578.5
356.84	1912.3	320.32	796.6	261.84	590.3
358.78	1310.9	325.27	823.8	266.80	605.3

Table S2 (Continued)

T / K	C_p / J K^{-1} mol^{-1}	T / K	C_p / J K^{-1} mol^{-1}	T / K	C_p / J K^{-1} mol^{-1}
271.76	618.7	374.73	876.2	43.51	97.36
276.72	633.2	377.70	884.4	45.35	98.87
281.68	646.8	380.66	890.3	47.21	102.1
286.63	668.3	383.62	890.9	49.07	103.6
291.59	685.0	386.58	904.3	50.94	105.4
296.54	697.6	389.53	914.3	53.26	109.0
301.50	713.3	392.48	918.3	56.03	109.5
306.45	732.5	Series 6		348.43	58.81
311.40	749.4	9.23	13.25	61.65	115.0
316.35	769.6	10.59	17.08	64.48	118.8
321.30	794.0	11.96	22.98	67.32	122.6
326.24	829.4	13.32	26.60	70.17	125.2
331.18	870.7	14.66	31.94	73.03	128.4
336.12	914.8	16.07	37.42	75.91	132.4
339.57	955.1	17.36	41.97	78.79	134.3
341.54	973.5	18.63	46.39	81.68	137.8
343.51	1000.2	19.88	52.81	84.58	142.8
345.48	1034.7	21.27	58.33	87.50	144.6
347.45	1091.5	22.49	64.34	90.41	149.8
349.42	1171.4	23.69	67.71	93.33	155.5
351.38	1324.4	24.85	76.35	96.26	159.4
353.31	1624.0	25.99	79.04	99.20	164.9
355.22	1964.0	27.15	78.09	103.09	173.1
357.13	1844.4	28.29	73.69	107.94	181.5
359.08	1229.6	30.92	79.39	112.80	189.5
361.08	1100.2	32.66	82.43	117.66	200.8
363.10	976.9	34.48	85.67	122.54	212.8
365.14	863.5	36.25	87.90	127.43	224.0
367.20	857.2	38.05	90.37	132.33	235.3
369.25	861.3	39.86	93.19	137.23	250.8
371.77	871.4	41.68	95.20	142.15	267.7

Table S2 (Continued)

T / K	C_p / J K^{-1} mol^{-1}	T / K	C_p / J K^{-1} mol^{-1}	T / K	C_p / J K^{-1} mol^{-1}
147.07	277.5	201.39	420.1	255.72	570.7
152.00	294.6	206.33	433.4	260.66	591.2
156.93	308.3	211.26	452.8	265.59	600.2
161.87	313.6	216.20	460.8	270.52	612.5
166.81	325.5	221.15	476.3	275.45	630.5
171.74	338.1	226.09	488.4	280.38	647.9
176.68	356.8	231.03	503.4	285.30	658.1
181.62	367.9	235.97	513.7	290.22	676.0
186.56	386.1	240.91	530.8	295.14	693.7
191.51	393.3	245.85	546.0	300.06	708.5
196.45	409.6	250.79	558.3		

References

1. H. Suzuki, M. Ishida, M. Yamashita, C. Otani, K. Kawachi, Y. Kasama and E. Kwon, *PCCP*, 2016, **18**, 31384-31387.
2. Y. Miyazaki, M. Sorai, R. Lin, A. Dworkin, H. Szwarc and J. Godard, *Chem. Phys. Lett.*, 1999, **305**, 293-297.